ADVANCED OPTICAL MATERIALS
www.advopticalmat.de

The Importance of Metal Ion Impurity Bands in the Photoluminescence of Halide Double Perovskites

Hei-Yui Kai, Daiwen Xiao, Ka-Leung Wong, Chang-Kui Duan, and Peter A. Tanner**

Double perovskite halides are attracting considerable attention due to their applications in solar cells and photovoltaics. It is observed that many (more than 20) publications in top journals have associated spectral features in emission in the region at 460–470 nm with "pristine" materials. This leads to not only false observations but also incorrect conclusions concerning the transformation of dark into bright excitons or boosting self-trapped exciton (STE) emission. The use of the phrase STE is commented upon. Most commonly, the spectra present correspond to those of the antimonate (III) ion, Sb^{3+}. The emission spectra should be interpreted in terms of sp–s^2 orbital transitions rather than self-trapped excitonic transitions. The compounds $Cs_2NaRECl_6$ (RE = Y, Gd) are synthesized by two major methods, namely: the evaporation and hydrothermal syntheses, for various rare earth starting materials, in order to demonstrate the effect of antimony contamination. Contamination by the Mn^{2+} ion is also found in the samples and double perovskite halides are susceptible to attack by moisture. This study emphasizes the need to check sample synthesis and sample purity and carefully monitor the integrity of starting materials.

1. Introduction

Optical emission spectra can be very sensitive to the presence of trace impurities coming from the starting materials or incorporated during synthesis. Although the impurity may be present in a small quantity, its emission can be enhanced by energy transfer from the host lattice or from the dominant chromophore to the impurity. Hence there are numerous examples in the literature showcasing both incorrect and questionable interpretations of bands in luminescence spectra. Some recent examples are the near-infrared emission of Fe^{3+} in $CaAl_{12}O_{19}$, which has been assigned to Bi^{3+},[1] and Mn^{2+}, and Fe^{3+} emission in stannates (assigned to oxygen vacancy generated states).[2] There are many other recent suspected cases, including the reported emission of Bi^{3+} in $LiGa_5O_8$[3] (due to Cr^{3+}) and of Cr^{3+} pairs in $LaMgGa_{11}O_{19}$[4] (due to Ni^{2+}), and Bi^{3+} emission in $ZnGa_2O_4$ (due to Cr^{3+}).[5] Hence, the optical spectra of major impurities such as Mn^{4+}, Cr^{3+}, and Fe^{3+} in particular need to be clearly understood and distinguished when reporting luminescence in the near-infrared region.

We focus on this Perspective in a case study involving pristine lead-free halide double perovskites, Cs_2NaMCl_6, where M is a trivalent transition metal or rare earth element, and it is situated at an octahedral site with chloride coordination (**Figure 1a**). Evidently, these materials are a hot topic, but unfortunately, inaccuracies and misconceptions have been promulgated throughout the literature and early studies of these systems (the so-called elpasolites) have been ignored. A Scopus search on 22 December 2024 identified 1925 papers concerning halide double perovskites thus far from 2023. Their importance is exemplified by Grandhi et al.,[6] who stated that lead-free perovskite-inspired materials with wide bandgap can offer a sustainable solution for the development of efficient tandem solar cells and photovoltaics. In this study, we identify impurities in the luminescence of pristine samples. We summarize in Table S1 (Supporting Information), the recently reported data in highly cited literature where the compounds reported as pure are in fact contaminated. In most cases, the pristine compounds are contaminated by Sb^{3+}, as shown in the Results section of this paper. We also clarify some of the terms and concepts employed in the literature which may be used in different contexts by materials scientists, chemists, and physicists. Our experimental results reinforce our arguments.

We focus upon the representative pristine system $Cs_2NaRECl_6$ (RE = rare earth), together with doping of antimony (Sb^{3+}) into the lattice. This is now discussed in detail. The RE^{3+} or Sb^{3+} ion is situated at an octahedral symmetry site, which endows

H.-Y. Kai, D. Xiao, K.-L. Wong, P. A. Tanner
Department of Applied Biology and Chemical Technology
The Hong Kong Polytechnic University
Hung Hom, Kowloon, Hong Kong SAR, P. R. China
E-mail: klgwong@polyu.edu.hk; monkey.tanner@polyu.edu.hk

C.-K. Duan
CAS Key Laboratory of Microscale Magnetic Resonance
and School of Physical Sciences
University of Science and Technology of China
Hefei 230026, P. R. China

C.-K. Duan
CAS Center for Excellence in Quantum Information and Quantum Physics
University of Science and Technology of China
Hefei 230026, P. R. China

The ORCID identification number(s) for the author(s) of this article can be found under https://doi.org/10.1002/adom.202500239

DOI: 10.1002/adom.202500239

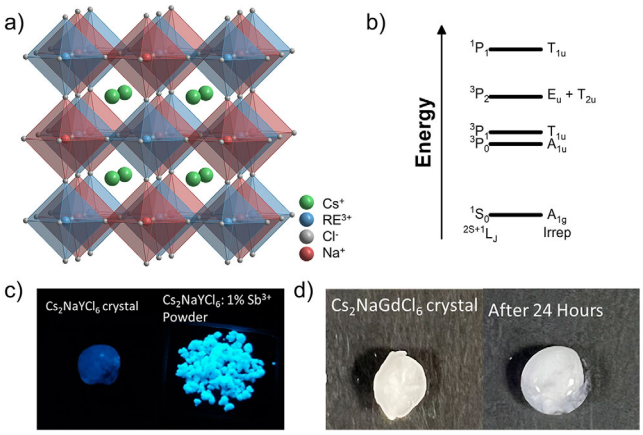

Figure 1. a) Structure of double perovskite (elpasolite) $Cs_2NaRECl_6$. RE blue; Na red; Cs green. b) Energy level diagram for an impurity ion with the ns^2 configuration in the gas phase (left) and in a crystal at an octahedral site (right side).[8] c) Photograph of emission from Cs_2NaYCl_6 and also doped with 1 at.% Sb, excited by 254 nm UV lamp radiation. d) Effect of exposure of $Cs_2NaGdCl_6$ crystal to ambient laboratory atmosphere, relative humidity 54%.

unique optical properties. The energy level scheme of the Sb^{3+} $[Kr]4d^{10}5s^2$ ion is shown in Figure 1b and has been the subject of previous careful studies.[7] and theoretical treatment.[8] With strong spin-orbit coupling, under O_h symmetry, the electronic ground state is $(^1S_0)A_{1g}$ and the excited states are $(^3P_0)A_{1u}$, $(^3P_1)T_{1u}$, $(^3P_2)E_u+T_{2u}$ and $(^1P_1)T_{1u}$ in order of increasing energy (Figure 1b). The transition to the lowest energy level $^1A_{1g} \rightarrow {}^3A_{1u}$ is electric dipole (ED) forbidden but can achieve vibronic intensity. The A absorption band, $^1A_{1g} \rightarrow {}^3T_{1u}$ (at ≈330 nm) is orbitally allowed, and spin-allowed via spin-orbit coupling with $^1P_1$. The B absorption band, $^1A_{1g} \rightarrow {}^3E_u+{}^3T_{2u}$ (at ≈280 nm) is only vibronically allowed, whereas the C band ($^1A_{1g} \rightarrow {}^1T_{1u}$ at ≈250 nm) is ED and spin allowed. The A and C bands are split by Jahn–Teller effects involving the e_g and t_{2g} vibrations. Just as for other ns^2 ions,[9] one would expect two strongly overlapping emission bands at low temperatures which are hardly distinguishable. In the case of $Cs_2NaLaCl_6$:Sb^{3+} only one broad emission band was reported in the blue spectral region at ≈470 nm.[7a] However, two emissive states from a tetragonal Jahn–Teller effect or crystal field splitting are deduced from lifetime measurements employing a variable magnetic field.[7b] The optical spectra are thus well understood from the works of Blasse and co-workers[7,10] to result from localized s^2–sp excitations of the Sb^{3+} ion within the $Cs_2NaLaCl_6$ lattice.

Some recent publications have attributed the emission of Sb^{3+} or Bi^{3+} diluted in halide double perovskites to be from self-trapped excitons (STEs).[11] It is important to clarify the meaning of STE and other terms in use. STEs are often viewed as the recombination of electrons and holes.[12a–d] When an exciton (which can be envisaged as an electron–hole pair) forms, the surrounding atoms in the lattice may shift and distort. This distortion could be so pronounced that the exciton is unable to escape from the "trap." STEs are found in materials that possess a soft lattice and as a result, the local lattice distortion can take place due to strong electron–phonon coupling, leading to the self-trapped state within the bandgap. Hence, a STE, essentially a localized exciton, has an emission peak below the free exciton emission peak. The emission intensity of a STE is mainly affected by the potential barrier and the transformation between the free exciton and STE. The extent of lattice distortion also determines the intensity of STE emission. STEs are characterized by broad peaks with large Stokes shifts.[12b,e] However, other types of transition – 4f–5d ED allowed transitions of lanthanide ions, for example– can also have broad peaks with large Stokes shifts. Unfortunately, the phrase STE is currently being applied in many cases to any broadband with a large Stokes shift, such as to an emission band of Sb^{3+} in Cs_2NaYCl_6 at 461 nm;[12f] the broad emission of Eu^{2+} impurity in $Cs_2NaEuCl_6$;[12g] the capping agent emission of $Cs_2NaYb_{0.94}Er_{0.06}Cl_6$ nanoparticles,[12h] etc. Oomen et al.[8c] have noted that the optical spectra of pristine $Cs_2NaSbCl_6$ result from $5s^2$–$5sp$ transitions of isolated Sb^{3+} ions, just as for Sb^{3+} doped into Cs_2NaMCl_6 (M = Y, La). The behavior of $Cs_2NaSbBr_6$ on the other hand, is explained by a semiconductor-type model so that the excitation spectrum corresponds to a band-to-band transition. In this case, the conduction band (CB) consists mainly of Sb^{3+} 5*p* character whilst the valence band (VB) consists of Sb^{3+} 5*s* character (both mixed to some extent with the 4*s* and 4*p* wavefunctions of Br). Hence the transition is actually the recombination of a Sb-5*s* hole in the VB with a Sb-5*p* electron in the CB and we have moved from a localized to a delocalized system.

We find that often the terms 'boosting the STE' or "turning dark STE into light STE"[13] have been employed in publications. In fact, what is happening is that a certain unrecognized impurity at trace amounts (such as Sb^{3+}) is present in the matrix to give broad, weak emission. Then the same ion has been added to the material to give much stronger emission at the same wavelength. In fact, as just mentioned, the emission is not from STE but from a luminescent impurity ion. Also, it is frequently reported that one or more potential energy curves of STEs in the bandgap are populated from Sb^{3+} levels, and then subsequently emit light, for example, refs. [12c,d]. It is the $^3P_{0,1} \rightarrow {}^1S_0$ transitions of Sb^{3+} which are luminescent.

The optical and other spectra of some pristine Cs_2MRECl_6 systems (M = Li, Na; RE = Y, La, Lu) are briefly reviewed in, Section S2 (Supporting Information).

In the next Section, following the brief experimental and characterization descriptions, we present our spectra of Sb^{3+} doped $Cs_2NaGdCl_6$ and show that many previous studies have erroneously confused this with "pristine" spectra.

It has been reported that these materials are stable in an ambient atmosphere for extended periods of time.[12c,13] Figure 1d shows the effect of ambient air at a relative humidity of 54% in our laboratory upon a crystal of $Cs_2NaGdCl_6$. The crystal is deliquescent and Cs_2NaYCl_6 is even more so.

2. Results and Discussion

2.1. Syntheses and Characterization

We have employed several methods to synthesize samples of $Cs_2NaRECl_6$ as detailed in the Experimental Section. First, Method A, the evaporation method consists of taking a concentrated HCl solution containing the reagent chemicals to dryness[14] (Morss Method E)[15] and protecting the resulting powder from exposure to moisture by adding nujol mineral oil.

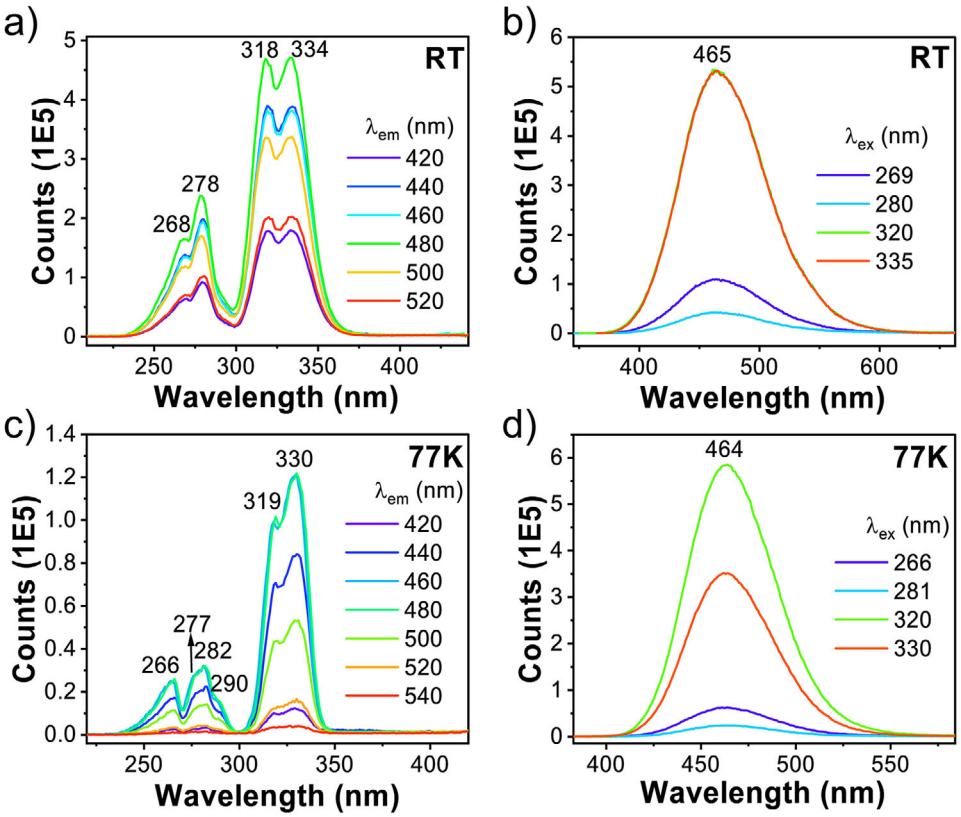

Figure 2. a) RT and c) 77 K excitation, and b) emission, d) spectra of $Cs_2NaGdCl_6$: Sb^{3+} (0.1 at.%) prepared by the evaporation method A.

Variants of this method included the addition of NH_4Cl into the starting solution (Method A1), and additionally when near dryness (Method A2), based upon the ammonium chloride route to anhydrous rare earth chlorides, to provide an additional Cl source because concentrated hydrochloric acid comprises only 37% HCl by mass.[16] Method B employed hydrothermal synthesis, adapted from ref. [17] We employed nitrate, chloride, and oxide rare earth starting materials, with similar results, and mainly report- those for the oxide materials. The analysis of starting materials was carried out by inductively coupled plasma–mass spectrometry (ICP-MS) using an indium internal standard. The results in, Section S3 (Supporting Information) show the presence of Mn and Sb at ppb levels. Samples were characterized by X-ray diffraction and X-ray photoelectron spectroscopy (Sections S4 and S5, Supporting Information).

2.2. Spectra of $Cs_2NaGdCl_6$ Samples Doped with Sb^{3+}

Figure 2 displays the excitation and emission spectra of samples of $Cs_2NaGdCl_6$ doped with 0.1 at.% Sb^{3+} at RT (a), (b) and 77 K (c), (d). The spectra of pure, undoped $Cs_2NaGdCl_6$ have previously been reported by de Vries and Blasse and we agree with their results for that spectral region.[10] The Gd^{3+} $^6P_{7/2} \rightarrow {}^8S_{7/2}$ emission band is observed at 314 nm. The RT emission of the 0.1 at.% Sb^{3+}-doped system recorded herein consists of a broad band in the blue spectral region, with the emission maximum at 465 nm. The excitation spectrum indicates a large Stokes shift, with the nearest features at ≈330, 320 nm. At room temperature, these bands are associated with the Jahn–Teller split $^3P_1$ excited state of Sb^{3+},[7b] so that the broad emission band corresponds to the vibronic structures of the spin-forbidden transition $^3T_{1u} \rightarrow {}^1A_{1g}$, Figure 1b. The full widths at half-maximum (FWHM) of the emission band at RT (Figure 2b) and 77 K (Figure 2d) are 83 and 53 nm. The $^3P_2$ levels (Figure 1b) lie at 290 nm and shorter wavelengths in Figure 2a,c. The results for the more highly doped system $Cs_2NaGdCl_6$:Sb^{3+} (1 at.%) are analogous and are included in, Figure S4 (Supporting Information). The emission decay results in Figure S5 (Supporting Information) indicate the mono-exponential Sb^{3+} lifetime at RT of 1.4 µs. This magnitude is appropriate for an electronic transition that is not first-order ED allowed.

The major conclusion here, in agreement with theoretical considerations, is that the broad emission band observed at 465 nm corresponds to *sp* emission from Sb^{3+}. Similar emission bands are observed for Sb^{3+} in other $Cs_2NaRECl_6$ systems. Many previous studies (for example, those listed in, Section S1, Supporting Information) have assigned similar emission and excitation bands to pristine $Cs_2NaRECl_6$ systems. We have examined pristine $Cs_2NaRECl_6$ systems, as reported in the following and we observe other impurity emission bands, as now discussed for the wavelength region 320–690 nm.

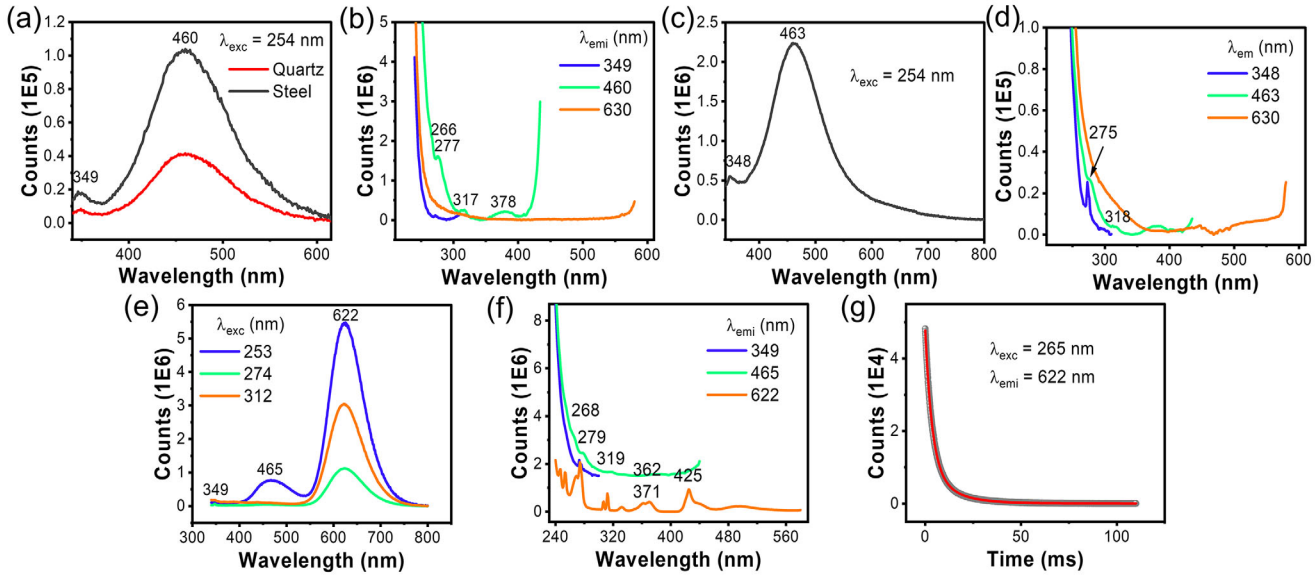

Figure 3. a–d) Spectra of $Cs_2NaGdCl_6$ prepared by Method A recorded by different sample holders (a) and instruments, using 254 nm excitation line (a),(c) and various emission lines (b),(d). The FL3 instrument was employed for (a),(b) whereas the FLS 1000 was used for (c),(d). Spectra of $Cs_2NaGd_{0.95}Mn_{0.05}Cl_6$ using several excitation lines e) and emission lines f) for the sample prepared by Method A; The spectra are displaced for clarity. g) Measurement of lifetime (black) with the biexponential fit (red): $\tau_1 = 3.6 \pm 0.0$ ms, $\tau_2 = 12.6 \pm 0.0$ ms, $R_{adj}^2 = 1.0000$. The FLS instrument was employed for recording (e)–(g).

2.3. Spectra of Pristine $Cs_2NaGdCl_6$ and Doped with Mn

It has been reported by that pure Cs_2NaYCl_6 crystals do not luminesce at RT under 365 nm excitation,[18] or $Cs_2NaLuCl_6$ crystals under 318 nm excitation,[19] or $Cs_2NaInCl_6$ nanocrystals under 280 nm excitation.[20a] Cs_2NaYCl_6 is transparent up to ≈45 000 cm^{-1}.[20b]

Following the detection of Mn from the ICP-MS results, we investigated the spectral consequence of adding Mn to $Cs_2NaGdCl_6$. Previous electron paramagnetic resonance studies have shown that Mn^{2+} substitutes at tetragonal sites in $Cs_2NaRECl_6$ either by substituting RE^{3+}[21a] or Na^+.[21b] The emission spectra of Cs_2NaYCl_6,[22] and $Cs_2Na_{1-x}Ag_xBiCl_6$[23] doped with Mn^{2+} have recently been reported and the $^4T_1 \rightarrow {}^6A_1$ transition is observed at 586–630 nm. Similarly, the emission is at 590 nm for $Cs_2NaBiCl_6$:Mn,[24] 583–614 nm in $Cs_2NaIn_xBi_{1-x}Cl_6$:Mn[25] and 632 nm for $Cs_2AgInCl_6$:Mn.[26]

The spectra of $Cs_2NaGdCl_6$ doped with 5% Mn prepared by the evaporation method were recorded using the FL3 and FLS1000 instruments with similar results. The emission bands in Figure 3e at 622, 460, and 349 nm correspond to Mn^{2+}, Sb^{3+}, and CsCl impurities, respectively, as shown by the excitation spectra, in Figure 3f. For example, the excitation spectral bands at 424, 371–362 nm are typical of Mn^{2+} emission, corresponding to the $^6A_1(^6S) \rightarrow {}^4E(^4G)$, $^4T_2(^4D)$, $^4E(^4D)$, transitions.[27] The measured lifetime of Mn^{2+} emission can be fitted by a biexponential function as shown in the caption and Figure 3g, or a monoexponential function with $\tau = 5.1$ ms, $R_{adj}^2 = 0.9941$.

The RT luminescence of pure CsCl has been reported previously.[28] The excitation spectrum shows a band peaking at 269 nm, and a broad emission band between 300 and 400 nm with the maximum at 335–360 nm,[28] in agreement with our results.

Our sample of undoped $Cs_2NaGdCl_6$ (**Figure 3a–d**) does not exhibit the Mn spectral features because the high intensity of Sb^{3+} bands masks them. However, the weak emission band at 349 nm indicates the presence of CsCl.

3. Take Home Messages

Halide double perovskites are regularly featured in current literature because they have important applications in upconversion, white light, photovoltaics, and solar cells. It is essential to understand their optical spectra so that applications can be tailored.

The phrase STE has a specific meaning and should not be applied indiscriminately to broad emission bands.

A major priority is sample purity and more attention is required for this. Even 99.999% purity starting materials have been shown to include adverse impurities. We find the presence of Mn and Sb in our chemicals and the Sb impurity gives rise to a spurious emission band which may involve incorrect interpretations.

The prevalent methods of synthesis of these materials by evaporation or hydrothermal synthesis are not optimal. The more time-consuming Bridgman method[15,29] was employed in the past but has gone out of favor. Our recommendations concerning the synthesis and handling of halide double perovskites are: i) take care of using high-purity starting materials; ii) employ Bridgman synthesis; iii) handle samples in a dry box; iv) check for spurious bands in emission spectra; v) analyze samples by ICP-MS; vi) perform careful optical experiments using different excitation and emission lines and measure emission lifetimes.

4. Experimental Section

Chemicals and Materials: Cesium chloride (CsCl, 99.999%), gadolinium (III) oxide (Gd_2O_3, 99.999%), and yttrium (III) oxide (Y_2O_3,

99.9999%) were purchased from Alfa Aesar. Hydrochloric acid (HCl, 37%) was purchased from RCI Labscan. Mineral oil (nujol oil), sodium chloride (99.999%), gadolinium (III) chloride hexahydrate $GdCl_3{\cdot}6H_2O$, 99.999%), yttrium (III) chloride hexahydrate ($YCl_3{\cdot}6H_2O$, 99.99%), and gadolinium (III) nitrate hexahydrate ($Gd(NO_3)_3{\cdot}6H_2O$, 99.999%) were purchased from Sigma–Aldrich. Yttrium (III) nitrate hexahydrate ($Y(NO_3)_3{\cdot}6H_2O$, 99.999%) was purchased from Strem Chemicals. The spectral results using $RECl_3$ and $RE(NO_3)_3$ (RE = Gd, Y) were similar and are not reported here. None of the above chemicals were further purified.

Synthesis of Halide Double Perovskites: Method A, For the synthesis of $Cs_2NaRECl_6$ powder the evaporation method was used. 1 mmol RE_2O_3 and 10 mL concentrated hydrochloric acid were added into a beaker and heated to 200 °C with stirring until the contents dissolved. Then 2 mmol CsCl, 1 mmol NaCl were also put into the beaker. This is solution A. The above mixture was put into an oil bath and heated to 160 °C with stirring until the hydrochloric acid completely evaporated. A white powder was formed. Nujol mineral oil was added to the powder sample to protect it from deliquescence. In Method A1, 0.1 mmol NH_4Cl was added to the solution A. In method A2, in addition to method A1, 0.1 mmol NH_4Cl was added to the almost dry mixture during evaporation and then, with mixing, taken to dryness.

Method B, hydrothermal synthesis of $Cs_2NaRECl_6$ crystals. 3 mmol RE_2O_3 was dissolved in 12 mL hydrochloric acid, and stoichiometric amounts of CsCl and NaCl were added after the solution became clear. The solution was transferred into a 25 mL Teflon-lined autoclave with a stainless-steel shell. Then, the autoclave was heated at 180 °C for 12 h in a furnace. The autoclave was slowly and steadily cooled to room temperature with a rate of 3 °C hr^{-1}. The crystals were collected and washed several times with isopropanol and then dried with tissue. Nujol mineral oil was added to cover the sample. In method B1, 0.3 mmol NH_4Cl was added to the initial solution. The results were similar and are not reported here.

Instruments: The X-ray diffraction (XRD) patterns of samples were collected by a Rigaku SmartLab 9 kW–Advance instrument using Cu$K\alpha$ radiation ($\lambda = 1.5418$ Å). X-ray photoelectron spectroscopy (XPS) was obtained using a Thermo Scientific Nexsa spectrometer. The emission, excitation spectra, and lifetime measurements at room temperature were recorded by an Edinburgh FLS1000 spectrometer, using a 450 W xenon lamp as the light source and a PMT-900 detector. A Fluorolog FL3 instrument was also alternatively employed. The spectra are uncorrected for instrument response. ICP-MS analysis was performed using an Agilent Technologies 7900 series ICP-MS instrument. The materials for ICP-MS measurements were prepared by dissolving 0.2 g of sample in 5 mL of concentrated nitric acid (70%, trace metal basis). 100 µL or 1 mL of the resulting solution was diluted with milli-Q water to reach the total volume of 10 mL for measurements.

Supporting Information

Supporting Information is available from the Wiley Online Library or from the author.

Acknowledgements

K.-L.W. acknowledges financial assistance from the Hong Kong Research Grants Council No. 12300021, NSFC/RGC Joint Research Scheme (N_PolyU209/21).

Conflict of Interest

The authors declare no conflict of interest.

Data Availability Statement

The data that support the findings of this study are available from the corresponding author upon reasonable request.

Keywords

antimony, double perovskite, elpasolite, excitation spectrum, photoluminescence

Received: January 22, 2025
Revised: March 13, 2025
Published online: March 25, 2025

[1] M. Liu, H.-Y. Kai, A. Huang, C.-K. Duan, K.-L. Wong, P. A. Tanner, *Chem. Mater.* **2023**, *35*, 2999.
[2] a) L. Lin, Q. Chen, Q. Zhang, J. He, H. Ni, J. Su, C.-K. Duan, *Chem. Mater.* **2024**, *36*, 10895; b) X. Ding, W. Zhou, H. Zhu, M. Cao, B. Yu, H. Cong, Q. Zhang, Y. Wang, *Laser Photonics Rev.* **2024**, *18*, 2300934; c) X. Qin, Y. Li, D. Wu, Y. Wu, R. Chen, Z. Ma, S. Liu, J. Qiu, *RSC Adv.* **2015**, *5*, 101347; d) X. Chen, Y. Li, K. Huang, L. Huang, X. Tian, H. Dong, R. Kang, Y. Hu, J. Nie, J. Qiu, *Adv. Mater.* **2021**, *33*, 2008722; e) J. Liu, Y. Liang, S. Yan, D. Chen, S. Miao, F. Xie, W. Wang, *J. Lumin.* **2022**, *251*, 119243; f) Y. Wang, W. Lei, S. Wu, F. Niu, Q. He, Y. Shen, F. Li, *Ceram. Int.* **2023**, *49*, 14426; g) Q. Chen, L. Lin, C. Ji, C. K. Duan, *Adv. Opt. Mater.* **2024**, *12*, 2401496.
[3] Z. Yi, P. Liu, X. Liu, Y. Xu, *Inorg. Chem.* **2023**, *62*, 19542.
[4] S. Liu, J. Du, Z. Song, C. Ma, Q. Liu, *Light Sci. Appl.* **2023**, *12*, 181.
[5] Z. Yi, P. Liu, Y. Xu, *Inorg. Chem.* **2023**, *62*, 9671.
[6] G. K. Grandhi, R. Dhama, N. S. M. Viswanath, E. S. Lisitsyna, B. Al-Anesi, J. Dana, V. Sugathan, H. Caglayan, P. Vivo, *J. Phys. Chem. Lett.* **2023**, *14*, 4192.
[7] a) E. Oomen, W. Smit, G. Blasse, *J. Phys. C: Solid State Phys.* **1986**, *19*, 3263; b) K. Meidenbauer, G. Gliemann, E. Oomen, G. Blasse, *J. Phys. C: Solid State Phys.* **1988**, *21*, 4703.
[8] a) P. Jacobs, *J. Phys. Chem. Sol.* **1991**, *52*, 35; b) M. Liu, C.-K. Duan, P. A. Tanner, C.-G. Ma, M. Yin, *J. Phys. Chem. C* **2021**, *125*, 26670; c) E. W. J. L. Oomen, W. M. A. Smit, G. Blasse, *Chem. Phys. Lett.* **1987**, *138*, 23.
[9] a) A. Fukuda, *J. Phys. Soc. Jpn.* **1976**, *40*, 776; b) A. Fukuda, P. Yuster, *Phys. Rev. Lett.* **1972**, *28*, 1032.
[10] A. de Vries, G. Blasse, *J. Chem. Phys.* **1988**, *88*, 7312.
[11] a) X. Li, D. Wang, Y. Zhong, F. Jiang, D. Zhao, S. Sun, P. Lu, M. Lu, Z. Wang, Z. Wu, *Adv. Sci.* **2023**, *10*, 2207571; b) Y. Jing, Y. Liu, M. Li, Z. Xia, *Adv. Opt. Mater.* **2021**, *9*, 2002213; c) A. Noculak, V. Morad, K. M. McCall, S. Yakunin, Y. Shynkarenko, M. Wörle, M. V. Kovalenko, *Chem. Mater.* **2020**, *32*, 5118; d) X. Li, H. Liang, C. Zheng, C. Zhao, S. Bai, X. Zhao, H. Zhang, Y. Zhu, *J. Alloys Compd.* **2023**, *966*, 171542; e) R. Zeng, L. Zhang, Y. Xue, B. Ke, Z. Zhao, D. Huang, Q. Wei, W. Zhou, B. Zou, *J. Phys. Chem. Lett.* **2020**, *11*, 2053; f) C. Wang, M. Sun, H. Wang, G. Zhao, *J. Phys. Chem. Lett.* **2022**, *14*, 164; g) B. Zhou, Z. Liu, S. Fang, J. Nie, H. Zhong, H. Hu, H. Li, Y. Shi, *J. Phys. Chem. Lett.* **2022**, *13*, 9140; h) F. Jiang, Z. Wu, M. Lu, Y. Gao, X. Li, X. Bai, Y. Ji, Y. Zhang, *Adv. Mater.* **2023**, *35*, 2211088.
[12] a) R. Williams, K. Song, *J. Phys. Chem. Sol.* **1990**, *51*, 679; b) K. S. Song, R. T. Williams, *Self-Trapped Excitons*, Springer, Berlin Heidelberg **2013**; c) G. Yang, S. Bai, X. Li, H. Liang, C. Li, J. Sun, Y. Wang, J. Huang, G. Pan, Y. Zhu, *ACS Appl. Mater. Interfaces.* **2023**, *15*, 24629; d) Y. Wang, S. Bai, J. Sun, H. Liang, C. Li, T. Tan, G. Yang, J. Wang, *J. Alloys Compd.* **2023**, *947*, 169602; e) B. Henderson, G. F. Imbusch, *Optical Spectroscopy of Inorganic Solids*, Oxford Science Publications, Oxford, England **2006**; f) Z. Rao, X. Zhao, X. Gong, *Adv. Func. Mater.* **2024**, *34*, 2406424; g) Z. Rao, X. Zhao, X. Gong, *Small* **2024**, *20*, 2406348; h) B. Kong, G. Pan, M. Wang, H. Tang, Z. Lv, S. Sun, Y. Luo, W. You, W. Xu, Y. Mao, *Adv. Sci.* **2025**, *12*, 2415473.
[13] X. Jiang, H. Ding, F. Yang, F. Luo, Z. Gan, Z. Fan, F. Gao, Z. Cheng, G. Luo, W. Zhou, *Inorg. Chem.* **2024**, *63*, 10756.

[14] P. Cresswell, D. Robbins, A. Thomson, *J. Lumin.* **1978**, *17*, 311.
[15] L. R. Morss, M. Siegal, L. Stenger, N. Edelstein, *Inorg. Chem.* **1970**, *9*, 1771.
[16] G. Meyer, P. Ax, *Mater. Res. Bull.* **1982**, *17*, 1447.
[17] H. Wang, J. Yao, Q. Wei, J. Zhao, B. Zou, R. Zeng, *Adv. Opt. Mater.* **2023**, *11*, 2300694.
[18] X.-X. Guo, J.-H. Wei, J.-B. Luo, Z.-L. He, Z.-Z. Zhang, J.-H. Chen, D.-B. Kuang, *Adv. Opt. Mater.* **2024**, *12*, 2301914.
[19] Y. Zhu, Y. Wang, Y. Sun, Z. Xu, M. Shang, *J. Lumin.* **2025**, *277*, 120909.
[20] a) Y. Yu, W. Zhou, C. Li, P. Han, H. Li, K. Zhao, *Nanomater.* **2023**, *13*, 549; b) K. Neuenschwander, H. U. Güdel, J. C. Collingwood, P. N. Schatz, *Inorg. Chem.* **1983**, *22*, 1712.
[21] a) R. Gleason, E. Muñoz P, J. Boldú, *J. Chem. Phys.* **1989**, *91*, 2776; b) C. Quintanar, R. Gleason, J. Boldú, E. Muñoz P, *J. Chem. Phys.* **1994**, *100*, 6979.
[22] S. Bai, H. Liang, C. Li, C. Tang, G. Yang, X. Xu, X. Yang, G. Pan, Y. Zhu, *Ceram. Int.* **2023**, *49*, 1102.
[23] M. Wang, J. Lyu, X. Qin, S.-W. Yang, X. Liu, G. Q. Xu, *J. Phys. Chem. Lett.* **2022**, *13*, 9429.
[24] J. D. Majher, M. B. Gray, T. A. Strom, P. M. Woodward, *Chem. Mater.* **2019**, *31*, 1738.
[25] P. Han, X. Zhang, C. Luo, W. Zhou, S. Yang, J. Zhao, W. Deng, K. Han, *ACS Cent. Sci.* **2020**, *6*, 566.
[26] K. Nila Nandha, A. Nag, *Chem. Commun.* **2018**, *54*, 5205.
[27] D. Curie, C. Barthou, B. Canny, *J. Chem. Phys.* **1974**, *61*, 3048.
[28] a) J. Kim, S. Ra, W. Kim, H. Kim, H. Park, S. H. Lee, H. Kang, S. Kim, D. Kim, S. Doh, *J. Korean Phys. Soc.* **2007**, *50*, 1514; b) H. Kimura, T. Kato, D. Nakauchi, M. Koshimizu, N. Kawaguchi, T. Yanagida, *Sens. Mater.* **2019**, *31*, 1265; c) J. Radhakrishnan, S. Selvasekarapandian, *J. Condens. Matter Phys.* **1994**, *6*, 6035.
[29] a) Z.-U. Hasan, F. S. Richardson, *Mol. Phys.* **1982**, *45*, 1299; b) A. Bessière, P. Dorenbos, C. Van Eijk, K. Krämer, H. Güdel, A. Galtayries, *J. Lumin.* **2006**, *117*, 187; c) P. A. Tanner, *Top. Curr. Chem.* **2004**, *241*, 167.